Oxidase-Loaded Hydrogels for Versatile Potentiometric Metabolite Sensing

Nicole L. Walker[a], **Jeffrey E. Dick**[a,b]

[a]Department of Chemistry, The University of North Carolina at Chapel Hill, Chapel Hill, NC 27599, USA

[b]Lineberger Comprehensive Cancer Center, School of Medicine, The University of North Carolina at Chapel Hill, Chapel Hill, NC 27599, USA

Abstract

Continuous monitoring of biological metabolites of interest necessitates sensors that are robust, versatile, miniaturizable, and reliable. Electrochemical biosensors have dominated the field of biosensors for decades due to their robust and inexpensive nature. Classically, these sensors use amperometric and voltammetric methods as the sensing modality. One of the greatest limitations with these methods is the dependence of the signal (current, i) on the electrode size, which can change with respect to time due to fouling. Here, we present open circuit potential, an electrochemical technique that is relatively insensitive to electrode size, as a reliable alternative to amperometric and voltammetric techniques for monitoring metabolites of interest. The sensor operates by trapping an oxidase enzyme in a chitosan hydrogel. The oxidase enzyme is required for metabolite specificity. When the oxidase enzyme meets its substrate, oxygen is consumed, and hydrogen peroxide is generated. Hydrogen peroxide generation dominates a half reaction at the platinum surface, resulting in a change in potential. Using the above criteria, we demonstrate the efficacy, long lifetime, sensitivity, and ease of fabrication of glucose sensors, and miniaturize the sensors from macro- to micro-electrodes. Additionally, we demonstrate the ease with which this platform can be extended to detect other analytes in the form of a galactose sensor. Our results set a foundation for the generalized use of potentiometric sensors for a broad range of metabolites and applications.

Keywords

Open circuit potential; biosensor; continuous glucose monitoring; glucose oxidase; galactose oxidase

1. Introduction

Diabetes is a metabolic disease that causes either low or high blood glucose levels, and is one of the leading causes of death in the world (Bollella et al., 2017; Heller and Feldman, 2010). In order to reliably monitor a diabetic's condition, continuous glucose monitoring in blood is required (Lee et al., 2019). Currently, commercial monitors are used, but they have to be replaced every 5–7 days as biofouling causes sensor performance to degrade over time (Nichols et al., 2013). Of the glucose monitoring systems that currently exist, most are electrochemical because electrochemistry is inexpensive, portable, rapid, simple for a non-scientist to operate, has high sensitivity and selectivity, and does not require sophisticated instrumentation (Ding and Qin, 2020; Guadarrama-Fernández et al., 2018).

While many electrochemical biosensors for glucose detection exist already, the vast majority of them are based on amperometry (Bollella et al., 2017; Luo et al., 2004; Pishko et al., 1991) or voltammetry (Rassas et al., 2019). Potentiometry is beneficial because, unlike voltammetry and amperometry, it uses a very high impedance, and so negligible current flows (Lee et al., 2019; Smith et al., 2020). As a result, interferent effects are reduced significantly and fouling of the sensor occurs at an incredibly slow rate (Smith et al., 2020) due to the insensitivity of potentiometry on electrode size (Park et al., 2013). This allows potentiometric sensors to be viable over extended time periods, making them quite enticing tools for situations that require continuous sensing, such as continuous glucose monitoring. Open circuit potentiometry in particular is tantalizing as it can be miniaturized quite easily without loss of sensitivity or the need for amplification strategies to detect the signal on micro- and nanoelectrodes.

Previously, potentiometric biosensors have been developed to address a variety of issues. Some are in the form of self-powering enzymatic fuel cells (Gu et al., 2019; Ohayon et al., 2020), others immobilize the biorecognition element on the channel of a field-effect transistor (Islam et al., 2020; Nakatsuka et al., 2018) or within an ion-selective membrane (Goud et al., 2020; Liu et al., 2020). However, the simplest type of biosensor to use and manufacture is one where the biorecognition element is immobilized on the surface of an electrode (Lee et al., 2019; Lv et al., 2018). The immobilization can be done in many ways, including the formation of a self-assembled monolayer (Lee et al., 2019) or entrapment in a hydrogel film (Luo et al., 2004; Pishko et al., 1991). The benefit of a hydrogel film over a self-assembled monolayer is that the self-assembled monolayer requires chemical alterations to the biorecognition element to immobilize it, which could lower its efficacy. Hydrogels, on the other hand, are formed by polymerizing a hydrophilic thin film onto the surface of the electrode, encapsulating the biorecognition element without chemically altering it in any way (Luo et al., 2004; Pishko et al., 1991). The reactants and products are able to diffuse throughout the hydrogel to react with both the biorecognition element and the electrode surface.

Enzymes are advantageous as a biorecognition element because they are specific, stable under biologically relevant conditions, reusable, relatively inexpensive to obtain, and there are thousands of options to choose from. There are three types of enzymatic biosensors that exist: first, second, and third generation (Bollella et al., 2017; Lee et al., 2019). First

generation biosensors use oxidoreductase enzymes as the biorecognition element, measuring either a decrease in oxygen content or an increase in hydrogen peroxide concentration to determine the concentration of the analyte. Second generation sensors do not probe dissolved oxygen content in solution, instead they probe electron transfer with respect to secondary redox mediators. Third generation biosensors avoid the need for any kind of mediator by using direct electron transfer enzymes as the biorecognition element. While these direct electron transfer-based biosensors are very effective and resistant to interferences (Lee et al., 2019), there are far fewer direct electron transfer enzymes available than oxidoreductase enzymes, though some oxidoreductase enzymes are capable of direct electron transfer behavior under the right conditions (Das et al., 2016). The online database for the Nomenclature Committee of the International Union of Biochemistry and Molecular Biology lists 1908 different enzymes under the category of oxidoreductase enzymes as of December 2020, but a cursory search of the direct electron transfer literature lists around 70 enzymes that have been observed to perform direct electron transfer (Gorton, 1999; Ghindilis, 1997; Ma, 2019; Okuda-Shimazaki, 2020). Additionally, enzymes need to be very close to the electrode surface for direct electron transfer to occur, but many of the enzymes trapped within a hydrogel would not be close enough to the electrode surface to function in this manner (Jenner and Butt, 2018). Similarly, though there are benefits to second generation sensors, the electron mediators used tend to be toxic to cells and add a further complication to the system.

In this study, we construct a simple, versatile, first-generation open circuit potentiometric biosensor by electrodepositing a polymer film of chitosan on the surface of an electrode in the presence of the enzyme glucose oxidase (GOx) (Figure 1a). GOx was chosen as the enzyme of choice as it is inexpensive, robust, and has a high turnover rate (Pishko et al., 1991). Chitosan was chosen to make the hydrogel because it is inexpensive, biocompatible, nontoxic, and forms films easily (Luo et al., 2004; Suginta et al., 2013). By applying a potential sufficient to reduce hydronium to hydrogen gas at the electrode surface, the pH of the chitosan solution begins to increase locally near the surface of the electrode. Once it surpasses the pKa of the amine groups, they begin to deprotonate, and the chitosan electropolymerizes and deposits on the electrode surface (Luo et al., 2004). When deposited in the presence of the enzyme, the chitosan encapsulates GOx near the electrode surface without chemical alterations. Finally, a layer of Nafion is added on top of the hydrogel to prevent enzyme leakage or detachment of the hydrogel, and to lessen the effects of interferents (Lee et al., 2019; Luo et al., 2004). We further demonstrate the efficacy of miniaturizing such sensors. To validate generalizability, we have constructed a sensor that can be easily modified to be selective for other metabolites of interest by switching GOx out for another oxidoreductase enzyme for the quantification of galactose.

2. Materials and methods

2.1. Chemicals and reagents

All chemicals were of analytical grade unless noted otherwise and were used as received. Glucose oxidase (GOx) from *Aspergillus niger* was obtained from MP Biomedicals. Dextrose (D-Glucose) (certified ACS granular powder) was obtained from Fischer

Bioreagents. Galactose oxidase from *Dactylium dendroides*, D-(+)-Galactose (99%), Chitosan (from shrimp shells, 75% (deacetylated)), 5% Nafion, L-Ascorbic Acid (99%), Acetaminophen (99%), ferricyanide (99.98%), and ferrocyanide (98.5 %) were obtained from Sigma-Aldrich. Hydrogen peroxide (30 wt%) was purchased from VWR International. Dulbeccos' Phosphate Buffered Saline (DPBS) (1X) with calcium and magnesium (pH = 6.8) was purchased from Corning. All stock solutions were made with DPBS.

2.2. Instrumentation

All open circuit potentiometry experiments were performed on a CHI model 601E or CHI 660D potentiostat (CH Instruments, Austin, TX). Deposition of the hydrogel film occurred on a CHI model 601E potentiostat using the amperometry technique. All stock solutions were prepared in DPBS (1X) and vortexed using a vortex-genie (Scientific Industries, New York, Bohemia). Platinum macroelectrodes (r = 1 mm) and platinum microelectrodes (r = 5 μm) were used as working electrodes. A silver/silver chloride reference electrode (stored in 1M KCl) and a glassy carbon rod as a counter electrode were used in every experiment. All electrodes were purchased from CHI (CH Instruments, Austin, TX).

2.3. Glucose sensor preparation

Chitosan was added to a solution of 1% (v/v) acetic acid in distilled water while stirring and gently heating until fully dissolved to make a 1% (w/v) chitosan solution. To make the deposition solution, 6.2 mg of GOx was suspended in 1 mL of 1% chitosan in 1% acetic acid and vortexed until homogeneous. Deposition of the hydrogel occurred by applying –0.50 V vs. Ag/AgCl for 7.5 minutes. The electrodes were then gently rinsed with ultrapure water and dried at room temperature. A protective layer of 10 μL of 1% Nafion (dissolved in ethanol) was drop cast onto the surface of the electrodes and allowed to dry at room temperature. The electrodes were stored in a refrigerator at 4 °C when not in use.

For the sensor on a microelectrode, the same procedure was done except that the deposition occurred for 1 minute and 3 μL 1% Nafion in ethanol was drop cast on top of the dried hydrogel.

2.4. Galactose sensor preparation

To make the deposition solution, 6.2 mg of galactose oxidase was suspended in 1 mL of 1% chitosan in 1% acetic acid and vortexed until homogeneous. Deposition of the hydrogel occurred by applying –0.50V vs. Ag/AgCl for 7.5 minutes. The electrode was then gently rinsed and dried at room temperature. A protective layer of 10 μL of 1% Nafion (dissolved in ethanol) was drop cast onto the surface of the electrode and allowed to dry at room temperature. The electrode was stored in a refrigerator at 4°C.

2.5. Glucose sensor optimization

Glucose sensors were prepared as described in section 2.3 on both macro- and microelectrodes using concentrations of GOx from 0 to 9.2 mg/mL. The sensors were then placed in stirred solutions of 50 μM glucose in PBS, and the open circuit potential was measured for 100 s. The biosensor with the strongest response to the glucose solution was taken as the ideal concentration of GOx for the biosensor (Supplementary Information, S1

and S2). For both macro- and microelectrodes, this was found to be 6.2 mg/mL. The ideal thickness was determined by a similar procedure where biosensors were prepared on both platinum macro- and microelectrodes as described in section 2.3 using the previously determined ideal GOx concentration and deposition times from 30 s to 15 minutes. The sensors were then placed in stirred solutions of 50 μM glucose in PBS, and an open circuit potential was taken for 100 s. The biosensor with the strongest response to the glucose solution was taken as the ideal deposition time (and therefore ideal hydrogel film thickness) for the biosensor (Supplementary Information, S3 and S4) and used for all future biosensor preparations. For both macroelectrodes, this was determined to be 7.5 minutes, while the ideal deposition time for microelectrodes was 1 minute.

2.6. Open circuit potentiometry procedure

Biosensors were rinsed gently with ultrapure water before and after every measurement. Open circuit potentiometry measurements were taken in a stirred solution of 10 mL of DPBS. An initial potential of 0.70 V was applied for 20 s to discharge any current that had built up on the surface of the electrode before the open circuit potentiometry measurement was taken (Lee et al., 2019; Reinmuth and Wilson, 1962). Following the end of the 20 s potential pulse, the potentiometric measurement began immediately. The open circuit potential was measured until a set start potential was reached, then the analyte was spiked in every 100 s. The recorded potential for each spike of analyte was the potential measured 100s after the spike occurred, regardless of if the potential had stabilized yet. The set start point was the potential where the baseline was achieved. For platinum macroelectrodes in solutions of DPBS only, the start potential was 0.43 V. For platinum macroelectrodes in solutions of DPBS containing acetaminophen and ascorbic acid, the start potential was 0.16 V. For platinum microelectrodes in solutions of DPBS, the start potential was 0.22 V.

3. Results and discussion

3.1. Development of the GOx-chitosan biosensor

The enzyme glucose oxidase (GOx) converts D-glucose to D-glucanolactone, reducing O_2 to H_2O_2 in the process. Therefore, as the concentration of glucose in the sample solution rises more H_2O_2 should be produced at the surface of the electrode (Figure 1b). We hypothesize that the presence of H_2O_2 at the electrode surface causes the open circuit potential to decrease because of concepts surrounding mixed potential theory, where in the absence of a strong redox couple, the potential of the system is determined by a weighted combination of the various components present in solution. (Park et al., 2013; Percival and Bard, 2017). To test this, an unmodified platinum macroelectrode was tested in a solution of Dulbeccos' Phosphate Buffered Saline (DPBS) with 1 μM to 3 mM H_2O_2 spiked in (Supplementary Information, S5). These experiments showed the same potential steps as seen on the GOx-chitosan electrode when the same concentrations of glucose are spiked into a DPBS solution (Figure 2a). This observation validates our claim that hydrogen peroxide is the dominant molecule that changes the interfacial potential.

Additionally, the results are in line with the general behavior that would be expected if H_2O_2 production is what is influencing the measured potential based on the Nernst equation: E_{OCP}

$= E_{eq} - (RT/nF)\ln(C_R/C_O)$. Here, E is the measured potential, E_{eq} is the equilibrium potential of the mixed system, R is the gas constant, T is the temperature in Kelvin, n is the moles of electrons involved in the redox reaction, F is Faraday's constant, C_O is the bulk concentration of the oxidant, and C_R is bulk the concentration of the reductant. As glucose concentration in solution rises, dissolved O_2 is being increasingly reduced to H_2O_2 by the enzymatic reaction. Thus, as more H_2O_2 is produced by the enzyme due to increased levels of glucose in solution, C_R raises and C_O lowers, leading to an overall decrease in the measured E value.

The open circuit potentiometric response of this GOx-chitosan electrode to glucose (Figure 2b) bears a similar shape to a binding isotherm. We developed a semiquantitative empirical model based off of mixed potential theory and Michaelis-Menten kinetics in order to describe this observed behavior. The specifics of the derivation can be found in the supplementary information, and the figure Supplementary Information, S6 demonstrates how closely the experimental and modelled data match.

Despite the use of semi-log plots being called into question recently (Clark and Dick, 2020, Urban, 2020), we decided to report both plots because the semi-log plot is common in the literature. Additionally, the logarithm of the function of the equation of the model described in the supplementary information should give linear regions where the concentration of the analyte is plus or minus an order of magnitude from K_M. As we see this behavior when the logarithm of the concentration of glucose is taken, the use of a semi-log plot is a suitable way to report this data. Using this semi-log plot, a calibration curve consisting of three linear ranges is identified. Figure 2c illustrates these 3 linear regions, from 1–10 μM, 10–100 μM, and 100 μM to 3 mM. The equations of each of these lines can be found in Supplementary Information, T1.

To evaluate the reproducibility, three platinum macroelectrodes were prepared in a batch together and tested by spiking glucose into solutions of DPBS (Figure 2d, log scale Supplementary Information S7). Each electrode exhibits a similar behavior up to 20 μM glucose. However, between 30 μM and 3 mM glucose added, the curves are statistically different according to a one-way ANOVA test (Supplementary Information, T2). This is due to slight differences in the electrode surfaces from the combination of miniscule variations in surface roughness, enzyme concentration in the hydrogel, hydrogel thickness, and thickness of the Nafion layer. These variations result in a relative standard deviation (%RSD) of 13.0% between all three electrodes. This is also demonstrated through the differences of the equations derived for the calibration curves for each of these electrodes (Supplementary Information, T1). This highlights the need to validate each biosensor before any measurement is taken, and optimization to increase interelectrode reproducibility will be the topic of a future investigation.

Though there is not much reproducibility between multiple electrodes made in the same way, repeated trials of the same electrode have very small %RSD values, between 2.83% and 4.50%. Thus, even for macroelectrode 2, which was tested 21 times over the course of 28 days, the behavior of a single biosensor is highly repeatable (Table 2) over an extended period of time.

To test the accuracy of these biosensors, a double-blind study was done in which one member of the lab made a solution of glucose in DPBS and the solution was tested by a different member with no knowledge of the solution's concentration. After the open circuit potential of a stirred solution of 10 mL of DPBS reached 0.43 V, 10 μL of the solution of unknown concentration was spiked into the DPBS. As seen in Table 2, there was a percent recovery of 112% for the measured unknown solution. This same procedure could be applied to a biofluid sample, as long as the calibrations were done in a matrix similar to that of the biofluid. The accuracy could be improved through the incorporation of electron mediators into the chitosan hydrogel, which would set the potential of the system and stabilize the biosensor response further. Biosensor improvements of this type will be a topic of future inquiry, and further details of this double-blind experiment are given in the supporting information.

3.2. Analysis of biosensor selectivity

The response to other common sugars was determined to evaluate selectivity of the biosensor. This was done by spiking in sucrose, lactose, or galactose in a solution of DPBS in the place of glucose. As can be seen in Figure 3a (log scale, Supplementary Information S8), the other sugars show a much lower binding affinity for the enzyme. For example, sucrose and lactose need to be present at 25–50 times the concentration of glucose in order to interfere, while galactose would need to be present at 13–50 times the concentration of glucose to interfere. Galactose interferes more strongly than lactose or sucrose does as it is structurally almost identical to glucose, differing only in the orientation of the hydroxyl group on carbon 4, while lactose and sucrose are disaccharides and much larger than the monosaccharide glucose. Importantly, these results indicate that in the presence of low concentrations of glucose, the sensor will respond exclusively to glucose.

We further demonstrate that other common interferents do not significantly affect the glucose sensing signal as long as they are present in both the calibration solution and the test samples. Glucose was spiked into a solution of DPBS containing biologically relevant levels of acetaminophen (1.3 mM) and ascorbic acid (170 μM) (Lee et al., 2019). As shown in Figure 3b (log scale, Supplementary Information S9), there is a shift in the linear range as compared to the calibration curves made in only DPBS. While the biosensor is less sensitive in the presence of these interferents, the biologically relevant glucose concentrations of ~3.9 mM to 10 mM (Bollella et al., 2017; Lee et al., 2019) are well within the linear range. Thus, the biosensor should be able to measure blood glucose levels without a need for sample dilution.

This shift in linear range and difference in open circuit potential response directionality can be explained by mixed potential theory (Percival and Bard, 2017). Without the interferants in solution, there is no redox mediator present to set a stable open circuit potential. However, the presence of redox active interferants is able to set the potential of the system, and they do so at a lower and more stable potential than is measured in DPBS alone. When H_2O_2 is produced at the electrode surface, it reacts with one or both of the interferents, causing an increase in the measured potential, as is predicted by the Nernst equation: $E_{OCP} = E_{eq} - (RT/nF)\ln(C_R/C_O)$. Here, E is the measured potential, E_{eq} is the equilibrium potential of the

mixed system, R is the gas constant, T is the temperature in Kelvin, n is the moles of electrons involved in the redox reaction, F is Faraday's constant, C_O is the bulk concentration of the oxidant, and C_R is bulk the concentration of the reductant. Since a combination of ascorbic acid and acetaminophen are participating in setting the potential of the system, the concentration of one or both of them is C_O. As the enzymatically produced H_2O_2 reacts with ascorbic acid and/or acetaminophen, the concentration of C_O decreases and the concentration of C_R increases, causing the measured potential to rise. As a result, the direction of the open circuit potential response is different in the presence of the interferants than it is when none are present. Further, a mixed potential will alter E_{eq}, which implies variation between measurements can be accounted for with mixed potential theory.

3.3. Analysis of biosensor stability

To test biosensor stability over long periods of time, one GOx-chitosan electrode was tested by repeated calibration over 28 days (Figure 2b). After 28 days, the electrode showed insignificant differences in the calibration curves obtained, with a % RSD of only 4.50%. The signal maintained 94%, 96%, and 97% of its original value for the first, second, and third linear regions, respectively, after 28 days and repeated use. These data indicate that there is very little change in sensor performance, even after nearly a month of use, and that the biosensor is useable for at least this length of time.

Additionally, another GOx-chitosan platinum macroelectrode was placed it in a 20 mL solution of 250 μM glucose in DPBS and the open circuit potential was recorded continuously over the course of 12 days, with a brief break in the middle at 6 days for the biosensor to be calibrated again. The calibration curves recorded for the electrode after 6 days and 12 days of the continuous measurement were statistically insignificant from the ones recorded beforehand (Figure 3c, log scale, Supplementary Information S10) according to an unpaired two-tailed T test (Supplementary Information, T3 and T4). The response of the biosensor maintained 100%, 87%, and 97% of its signal for the first, second, and third linear regions, after 12 days of continuous use.

The results from this study are compared to other, similar potentiometric biosensors for glucose detection in Table 1. This shows that the main advantage of this biosensor over others is the signal stability over longer periods of time, maintaining nearly the same signal over the course of a month of repeated testing and over 12 days of continuous use. Additionally, compared to most of the other similar biosensors, it is faster and easier to fabricate. While the upper limit of the linear range(s) is much lower here than in most of the other biosensors, the lower limit is either better or comparable. The main disadvantage is background stability, which can be optimized by incorporating redox molecules with fast heterogeneous electron transfer kinetics in the hydrogel.

3.4. Miniaturization of the glucose biosensor to a microelectrode

The ability to miniaturize sensors is important for continuous monitoring purposes and the comfort of the patient. To validate the ease of biosensor miniaturization, we fabricated the GOx-chitosan sensor on a platinum microelectrode ($r = 5$ μm). As can be seen in Figure 4 (log scale, Supplementary Information S11), the GOx-chitosan platinum microelectrode

biosensor responds to spikes of glucose in a similar manner to the macroelectrode biosensor. Like the biosensor on the macroelectrode, there are three linear regions present when the log of the glucose concentration is taken (Supplementary Information, T5), and the %RSD of repeated calibrations of the same electrode is low (Table 2). Notably, the GOx-chitosan platinum microelectrode responds to a larger range of glucose concentrations than the platinum macroelectrode, and the potentials measured are not the same.

The differences between the open circuit potentiometric response of the GOx-chitosan biosensor on a microelectrode and a macroelectrode are believed to be the results of mixed potential theory. When the open circuit potential of a bare platinum macroelectrode and microelectrode in DPBS are compared, there is a clear difference in potentiometric response based on the size of the electrodes (Supplementary Information, S12), implying that there is a size component to a mixed potential system. We note that the difference in potential is 0.15 V, whereas the difference in current expected between the two different sized electrodes is 10^3 A. Thus, the potentiometric sensing is insensitive to electrode size. However, when a redox couple, such as ferricyanide/ferrocyanide is present in solution, mixed potential theory no longer applies and the open circuit potential is the same, regardless of the size of the electrode (Supplementary Information, S13). Thus, we hypothesize that the proposed addition of electron mediators to the chitosan hydrogel will not only improve biosensor accuracy as discussed above, but it will also result in a lack of significant difference between the open circuit potential response of the biosensor regardless of electrode size.

3.5. Demonstration of versatility using galactose oxidase

In order to demonstrate the versatility of this type of sensor, a biosensor for galactose was made by swapping the GOx enzyme for galactose oxidase. This enzyme converts D-galactose to D-galacto-hexodialdose, forming H_2O_2 as a byproduct. In the same manner that the glucose sensor uses the production of H_2O_2 to alter the potential of the electrode surface and causes a decrease in observed open circuit potential, the galactose biosensor uses the enzymatic production of H_2O_2 in the presence of D-galactose to lower the electrode's surface potential. As can be seen in Figure 5 (log scale, Supplementary Information S14), the galactose oxidase sensor is less sensitive and has a wider linear range than that of the GOx biosensor. This is because of the higher rate of turnover of glucose oxidase, which has a k_{turn} of ~1000 s^{-1} (Pishko et al., 1991). Since galactose oxidase has a slower turnover rate than GOx does ($k_{turn} = 650$ s^{-1} (Tressel and Kosman, 1982)), it takes a larger concentration of analyte to produce the enough H_2O_2 to alter the potential of the electrode to the same degree. The three linear regions present when the log of the galactose concentration is taken are listed in Supplementary Information, T6, and the %RSD of repeated calibrations of the same electrode is presented in Table 2.

4. Conclusion

In this study, we developed a simple, versatile open circuit potentiometry glucose sensor that is stable over long time periods. Even after repeated use over the course of 28 days and continuous use over 12 days, the sensors maintain their performance. These biosensors are easy and inexpensive to create, and are simple to miniaturize or to make selective for other

metabolites. While the presence of interferents influences the sensor response, calibration of the sensor in the presence of the interferents solves this issue. This work lays a foundation for versatile metabolite sensing using potentiometry. Potentiometry is powerful due to its insensitivity to electrode size, indicating adsorbates do not interfere with the sensor sensitivity over long periods of time. This type of sensor is imperative for wearable and implantable sensors in complex matrices.

Supplementary Material

Refer to Web version on PubMed Central for supplementary material.

Acknowledgements

References

Bollella P, Gorton L, Ludwig R, Antiochia R, 2017. Sensors. 17, 1912.

Clark RB, Dick JE, 2020. ACS Sens. 5, 3591–3598. [PubMed: 33169613]

Das P, Das M, Chinnadayyala SR, Singha IM, Goswami P, 2016. Biosens. Bioelectron 79, 386–397. [PubMed: 26735873]

Ding J, Qin W, 2020. Trends Anal. Chem 124, 115803.

Ghindilis AL, Atanasov P, Wilkins E, 1997. Electoranal. 9, 661–674.

Gorton L, Lindgre A, Larsson T, Munteanu FD, Ruzgas T, Gazaryan I, 1999. Anal. Chim. Acta 400, 91–108.

Goud KY, Teymourian H, Sandhu SS, Tostado N, Mishra RK, Moore LC, Harvey SP, Wang J, 2020. Sens. Actuators B Chem 320, 128344.

Gu C, Kong X, Liu X, Gai P, Li F, 2019. Anal. Chem 91, 8697–8704. [PubMed: 31247724]

Guadarrama-Fernández L, Novell M, Blondeau P, Andrade FJ, 2018. Food Chem. 265, 64–69. [PubMed: 29884395]

Heller A, Feldman B, 2010. Acc. Chem. Res 43, 963–973. [PubMed: 20384299]

Islam AE, Martineau R, Crasto CM, Kim H, Rao RS, Maruyama B, Kim SS, Drummy LF, 2020. ACS Appl. Nano Mater 3, 5088–5097.

Jenner LP, Butt JN, 2018. Curr. Opin. Electrochem 8, 81–88.

Lee I, Loew N, Tsugawa W, Ikebukuro K, Sode K, 2019. Biosens. Bioelectron 124–125, 216–223.

Liu Y, Cánovas R, Crespo GA, Cuartero M, 2020. Anal. Chem 92, 3315–3323. [PubMed: 31971373]

Luo XL, Xu JJ, Du Y, Chen HY, 2004. Anal. Biochem 334, 284–289. [PubMed: 15494135]

Lv E, Ding J, Qin W, 2018. Sens. Actuators B Chem 259, 463–466.

Ma S, Ludwig R, 2019. ChemElectroChem 6, 958–975. [PubMed: 31008015]

Nakatsuka N, Yang KA, Abendroth JM, Cheung KM, Xu X, Yang H, Zhao C, Zhu B, Rim YS, Yang Y, Weiss PS, Stojanovi MN, Andrews AM, 2018. Science. 362, 319. [PubMed: 30190311]

Nichols SP, Koh A, Storm WL, Shin JH, Schoenfisch MH, 2013. Chem. Rev 113, 2528–2549. [PubMed: 23387395]

Ohayon D, Nikiforidis G, Savva A, Giugni A, Wustoni S, Palanisamy T, Chen X, Maria IP, Di Fabrizio E, Costa PMFJ, McCulloch I, Inal S, 2020. Nat. Mater 19, 456–463. [PubMed: 31844278]

Okuda-Shimazaki J, Yoshida H, Sode K, 2020. Bioelectrochem. 132, 107414.

Park JH, Zhou H, Percival SJ, Zhang B, Fan FRF, and Bard AJ, 2013. Anal. Chem 85, 964–970. [PubMed: 23240811]

Percival SJ, Bard AJ, 2017. Anal. Chem 89, 9843–9849. [PubMed: 28825303]

Pishko MV, Michael AC, Heller A, 1991. Anal. Chem 63, 2268–2272. [PubMed: 1759711]

Ramašauskas L, Meškys R, Ratautas D, 2020. Biosens. Bioelectron 164, 112338. [PubMed: 32553347]

Rassas I, Braiek M, Bonhomme A, Bessueille F, Raffin G, Majdoub H, Jaffrezic-Renault NAO, 2019. Sensors. 19, 154.

Reinmuth WH, Wilson CE, 1962. Anal. Chem 34, 1159–1161.

Smith LA, Glasscott MW, Vannoy KJ, Dick JE, 2020. Anal. Chem 92, 2266–2273. [PubMed: 31830783]

Song Y, Su D, Shen Y, Liu H, Wang Li., 2017. Anal. Bioanal. Chem 409, 161–168. [PubMed: 27730259]

Suginta W, Khunkaewla P, Schulte A, 2013. Chem. Rev 113, 5458–5479. [PubMed: 23557137]

Tressel PS, Kosman DJ, 1982. Method Enzymol. 89, 163–171.

Urban PL, 2020. Anal. Chem 92, 10210–10212. [PubMed: 32649180]

Ali SMU, Nura O, Willander M, Danielsson B, 2010. Sens. Actuators B 145, 869–874.

Highlights

- Developed a simple, versatile potentiometric biosensor for small molecule metabolite quantification

- Generalizable to any small molecules that reacts with an oxidase enzyme

- Open circuit potentiometry is insensitive to electrode size, unlike amperometry and voltammetry

- Miniaturization to micro/nanosensors is achievable

a) pH 2.4 → pH 6.3 | 2H+ H₂ | 2H+ H₂ | b) O₂ + | + H₂O₂

Initial Chitosan Film Formation | Build-up of Chitosan Film | Final Chitosan Hydrogel Structure

Key: = Chitosan = Glucose oxidase = D-glucose = D-gluconolactone
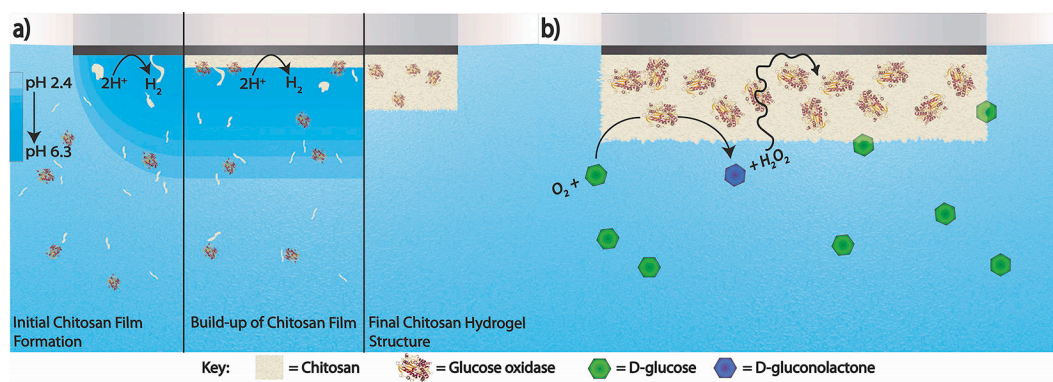
Figure 1.
a) The formation of the GOx-chitosan hydrogel on the surface of a platinum electrode through the electrodeposition of chitosan in the presence of GOx. **b)** The reaction that occurs on the surface of the GOx-chitosan platinum electrode to alter the surface potential. Glucose is oxidized to glucanolactone in the presence of O_2, forming H_2O_2 as a byproduct. The H_2O_2 in the hydrogel then alters the measured open circuit potential.
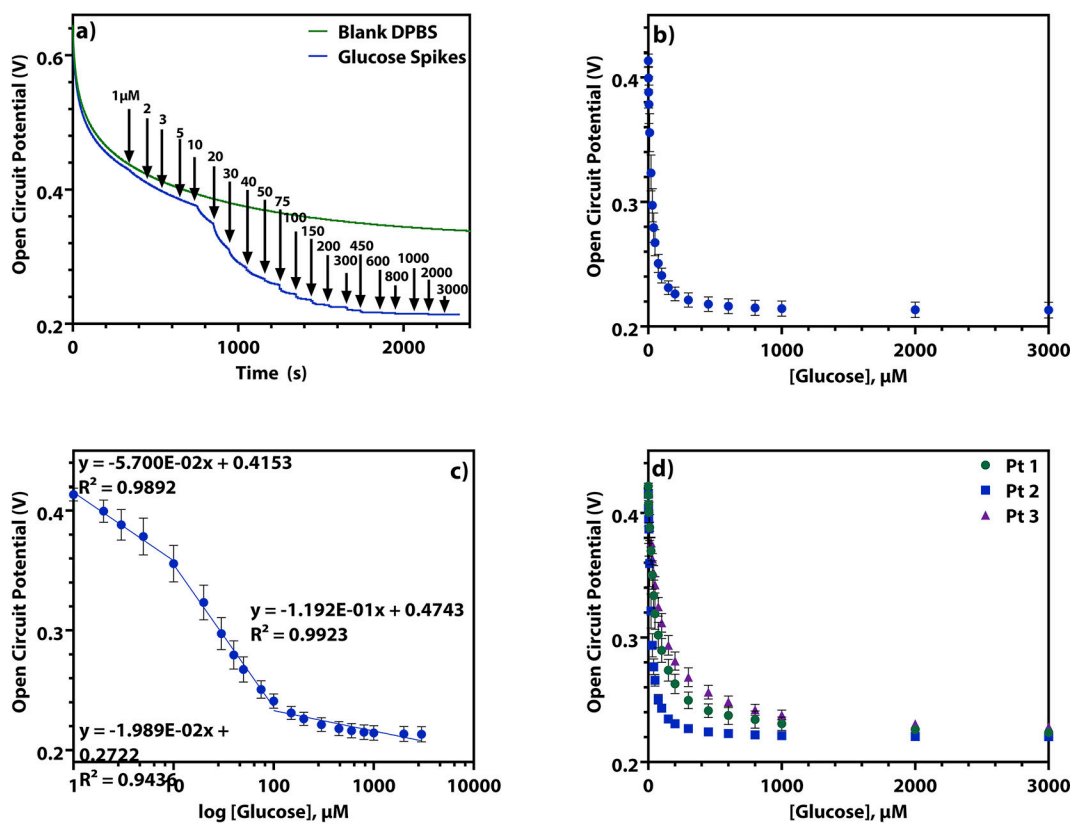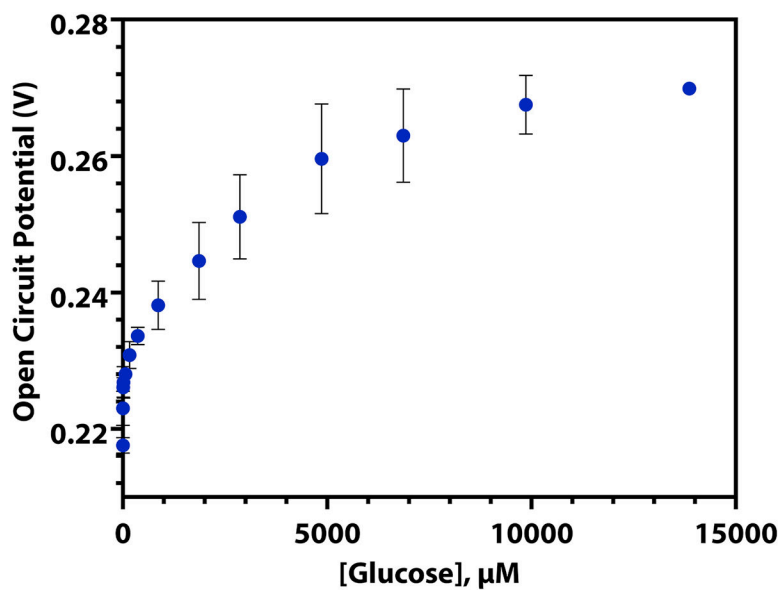
Figure 2.
a) The open circuit potential of a GOx-chitosan platinum macroelectrode in (green) a blank solution of DPBS and (blue) as 1μM to 3mM glucose is spiked into a solution of DPBS. **b)** The open circuit potential of a GOx-chitosan platinum macroelectrode as 1 μM to 3 mM glucose is spiked into a solution of DPBS over 28 days (n = 21, RSD = 4.50%). **c)** The semi-log plot of the open circuit potential of a GOx-chitosan platinum macroelectrode as 1 μM to 3 mM glucose is spiked into a solution of DPBS over 28 days (n = 21, RSD = 4.50%). **d)** The open circuit potential of 3 GOx-chitosan platinum macroelectrodes as 1 μM to 3 mM glucose is spiked into a solution of DPBS (n = 3, each).
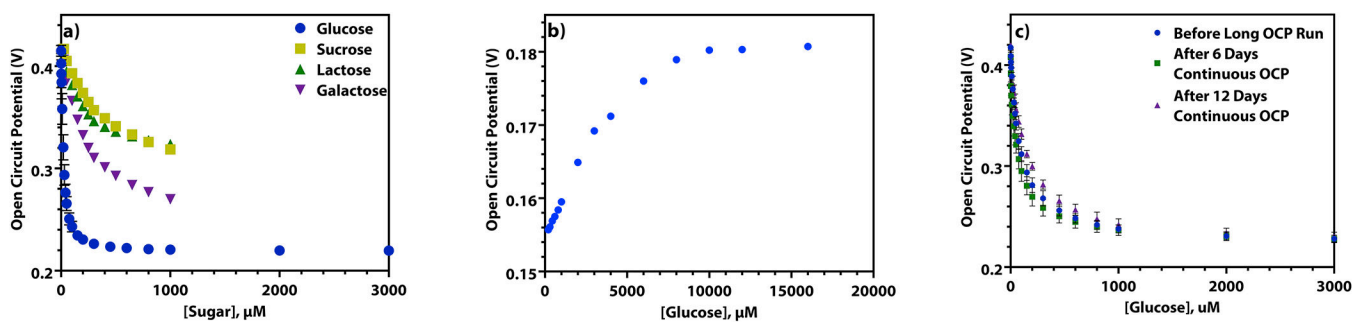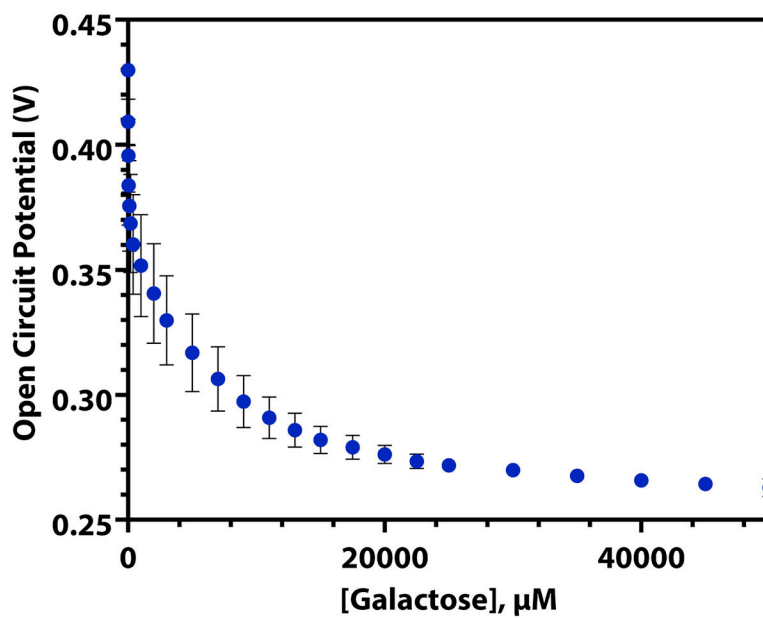
Figure 3.

a) The open circuit potential of a GOx-chitosan platinum macroelectrode as 1 μM to 3 mM different sugars are spiked into a solution of DPBS (n = 3). **b)** The open circuit potential of a GOx-chitosan platinum macroelectrode as 200 μM to 18 mM glucose is spiked into a solution of DPBS containing 1.3 mM acetaminophen and 170 μM ascorbic acid. **c)** The experimental open circuit potential (n = 3) of a GOx-chitosan platinum macroelectrode when 1 μM to 3 mM glucose is spiked into a solution of DPBS (**blue**) before being used in a continuous measurement, (**green**) after being used in a continuous measurement for 6 days, and (**purple**) after being used in a continuous measurement for 12 days.

Figure 4.
The open circuit potential of a GOx-chitosan platinum microelectrode as 1 μM to 14 mM glucose is spiked into a solution of DPBS (n = 3, RSD = 3.10%).

Figure 5.
The open circuit potential of a galactose oxidase-chitosan platinum macroelectrode as 10 μM to 50 mM galactose is spiked into a solution of DPBS (n = 3, RSD = 5.84%).

Table 1.

Comparison of biosensor to similar potentiometric biosensors for glucose detection

Materials	ZnO nanowires, Nafion, GOx	4-MBA[a], AuNPs[b], GDH[c]	KSC[d], GOx	DSH[e], DET-FADGDH[f]	Chitosan, Nafion, GOx
Type of Enzyme Immobilization	Crosslinked to nanowires	Self-assembled monolayer	Adsorbed into KSC pores	Self-assembled monolayer	Hydrogel
Biosensor Generation	First	Third	First	Third	First
Ease of Fabrication	Moderate	Moderate	Moderate	Easy	Easy
Fabrication time	~ 3 hours	~ 1 day	~ 14 hours	~ 2 days	~ 1 hour
Linear Range (s)	0.5 – 1000 μM	1–8 mM	0.03 – 10 mM	1 – 500 μM, 0.5 – 50 mM, 50 –200 mM	1–10 μM, 10–100 μM, 100–3000 μM
Lifetime	21 days	10 days	15 days	9 days (continuous)	28 days
Reference	Ali et al., 2010	Ramašauskas et al, 2020	Song et al., 2017	Lee et al., 2019	This work

[a]4-MBA = 4-mercaptobenzoic acid

[b]AuNPs = gold nanoparticles

[c]GDH = glucose dehydrogenase

[d]KSC = macroporous carbon derived from kenaf stem

[e]DSH = Dithiobis(succinimidyl hexanoate)

[f]DET-FADGDH = direct electron transfer FAD-dependent glucose dehydrogenase

Table 2.

Figures of merit for the GOx-chitosan electrodes on platinum macroelectrodes and microelectrodes, and for the galactose oxidase-chitosan electrodes on platinum macroelectrodes

Electrode	Macro 1 (GOx)	Macro 2 (GOx)	Macro 3 (GOx)	Micro 1 (GOx)	Macro 4 (galactose oxidase)
%RSD (n = 3)	3.93	4.66 (n = 18)	2.83	3.10	5.84
%RSD	13.0			-----	-----
% Recovery	-----	112	-----	-----	-----